Genomic architecture of Shh dependent cochlear morphogenesis

Victor Muthu[1], Alex. M. Rohacek[1], Yao Yao[2], Staci M. Rakowiecki[1], Alexander S. Brown[1], Ying-Tao Zhao[1], James Meyers[1], Kyoung-Jae Won[3], Shweta Ramdas[1], Christopher D. Brown[1], Kevin A. Peterson[4], and Douglas J. Epstein[1,5].

[1]Department of Genetics, Perelman School of Medicine, University of Pennsylvania, Philadelphia, Pennsylvania, USA. [2]Department of Animal and Dairy Science, Regenerative Bioscience Center, University of Georgia. [3]Biotech Research and Innovation Centre (BRIC), Novo Nordisk Foundation Center for Stem Cell Biology, DanStem, Faculty of Health and Medical Sciences, University of Copenhagen, Copenhagen N, Denmark. [4]The Jackson Laboratory, Bar Harbor, Maine, USA.

[5]Corresponding Author: Douglas J. Epstein, Ph.D.
Professor and Vice Chair
Department of Genetics
Perelman School of Medicine
University of Pennsylvania
Clinical Research Bldg., Room 463
415 Curie Blvd
Philadelphia, PA 19104
Phone: (215) 573-4810
Email: epsteind@pennmedicine.upenn.edu

Running title: Regulation of cochlear duct outgrowth

Key Words: cochlea, organ of Corti, otic vesicle, sensory development, gene regulation, Shh signaling

SUMMARY STATEMENT

An integrated genomic approach identifies Shh responsive genes and associated regulatory sequences with known and previously uncharacterized roles in cochlear morphogenesis, including genes that prime the cochlea for sensory development.

ABSTRACT

The mammalian cochlea develops from a ventral outgrowth of the otic vesicle in response to Shh signaling. Mouse embryos lacking Shh or its essential signal transduction components display cochlear agenesis, however, a detailed understanding of the transcriptional network mediating this process is unclear. Here, we describe an integrated genomic approach to identify Shh dependent genes and associated regulatory sequences that promote cochlear duct morphogenesis. A comparative transcriptome analysis of otic vesicles from mouse mutants exhibiting loss (*Smo*^{ecko}) and gain (*Shh-P1*) of Shh signaling revealed a set of Shh responsive genes partitioned into four expression categories in the ventral half of the otic vesicle. This target gene classification scheme provided novel insights into several unanticipated roles for Shh, including priming the cochlear epithelium for subsequent sensory development. We also mapped regions of open chromatin in the inner ear by ATAC-seq that, in combination with Gli2 ChIP-seq, identified inner ear enhancers in the vicinity of Shh responsive genes. These datasets are useful entry points for deciphering Shh dependent regulatory mechanisms involved in cochlear duct morphogenesis and establishment of its constituent cell types.

INTRODUCTION

The mammalian cochlea derives from a ventral extension of the otic vesicle. Over the course of several days during embryonic development, this outgrowth undergoes a complex sequence of morphogenetic changes resulting in cochlear lengthening, coiling and differential patterning into sensory and nonsensory cell types that are essential for hearing (Wu and Kelley 2012; Basch et al., 2016; Montcouquiol and Kelley, 2019). Congenital malformations of the cochlea or defects in many of its constituent cell types are primary causes of hearing loss, emphasizing the importance of a thorough understanding of cochlear development (Jackler et al., 1987; Dror and Avraham, 2010; Schwander et al., 2010; Korver et al., 2017).

The organ of Corti is a specialized sensory structure for hearing in mammals that lines the length of the cochlear duct. It comprises a single row of inner hair cells (IHCs), three rows of outer hair cells (OHCs) and a variety of interspersed support cells that sit atop the basilar membrane. Sound waves are propagated through the cochlear duct by way of fluid motions that cause the basilar membrane to resonate at frequency dependent positions. OHCs enhance hearing sensitivity and frequency selectivity by amplifying basilar membrane vibrations in a feedback loop driven by OHC electromotility (Fettiplace 2017). Excitation of IHCs convert sound induced vibrations into electrochemical signals that are transmitted to the brain along auditory nerve fibers (Kazmierczak and Muller, 2012; Yu and Goodrich, 2014). Even slight deviations in the precise arrangement of sensory and non-sensory cell types in the organ of Corti can alter auditory perception (Montcouquiol and Kelley, 2019).

We previously described a critical function of the Sonic hedgehog (Shh) signaling pathway in promoting ventral identity within the otic vesicle that is necessary for the initiation of cochlear duct outgrowth (Riccomagno et al., 2002; Bok et al., 2007; Brown and Epstein, 2011). Mouse embryos lacking *Shh*, or carrying an ear conditional knockout of *Smoothened* (*Foxg1cre; Smo*$^{loxp/-}$, herein termed *Smo*^{ecko}), an essential Shh signal transduction component, exhibit cochlear agenesis. We also classified several transcription factors (*Pax2, Otx2, Gata3*) with key roles in cochlear development as transcriptional targets of Shh signaling within the ventral otic epithelium (Brown and

Epstein, 2011). Despite these advances, a detailed understanding of the mechanism by which Shh dependent transcription factors promote cochlear duct outgrowth remains unclear, in part, because the genes acting downstream in this transcriptional cascade have yet to be fully elucidated.

Shh regulates the expression of target genes through the Gli family of zinc finger containing transcription factors (Falkenstein and Vokes, 2014). In response to Shh signaling, transcription can be activated by the binding of full-length Gli proteins (Gli1, Gli2, Gli3) to cognate recognition sequences in the enhancers and promoters of target genes, often in conjunction with cooperating factors, or alternatively, by preventing the accumulation of a truncated Gli3 repressor (Bai et al., 2004; Peterson et al., 2012; Oosterveen et al., 2012; Oosterveen et al., 2013; Falkenstein and Vokes, 2014). Cochlear duct outgrowth is severely impaired in *Gli2*$^{-/-}$*;Gli3*$^{-/-}$ embryos and is not effectively restored in *Shh*$^{-/-}$*;Gli3*$^{-/-}$ double mutants (Bok et al., 2007). These genetic data suggest that Gli2 and Gli3 function primarily as transcriptional activators to promote the extension of the cochlear duct (Bok et al., 2007). However, as with the other Shh dependent transcription factors mentioned above, the inner ear specific targets of Gli2 and Gli3 remain unknown.

To identify novel targets of Shh signaling in the inner ear we performed RNA-seq on otic vesicles isolated from mouse mutants displaying a loss (*Smo*^{ecko}) or gain (Shh-P1) in Shh signaling at E11.5, when cochlear outgrowth is first evident. We uncovered an intriguing set of Shh responsive genes with known and previously uncharacterized roles in cochlear morphogenesis. We also mapped regions of open chromatin in the inner ear by ATAC-seq (assay for transposase-accessible chromatin using sequencing) that, in combination with Gli2 ChIP-seq, identified inner ear enhancers in the vicinity of Shh responsive genes, several of which were functionally validated *in vivo* using a mouse transgenic reporter assay. This integrated genomic approach revealed several unexpected roles for Shh signaling, including transcriptional regulation of a set of genes that prime the medial wall of the cochlear duct for subsequent sensory development.

RESULTS

Screening for Shh responsive genes expressed during cochlear duct outgrowth

To identify a comprehensive set of genes regulated by Shh signaling at early stages of cochlear duct outgrowth we performed RNA-seq on otic vesicles isolated at E11.5 from two different mouse mutants and corresponding control littermates that were previously shown to exhibit loss (*Smo*^{ecko}) and gain (*Shh-P1*) of Shh signaling in the otic epithelium (Riccomagno et al., 2002; Brown and Epstein, 2011). *Shh-P1* embryos display ectopic expression of *Shh* in the dorsal otic vesicle from a P1 transgene (Riccomagno et al., 2002). A total of 1,122 genes (581 downregulated, 541 upregulated) were differentially expressed between *Smo*^{ecko} and control otic vesicles (FDR≤0.05 and RPKM≥1.0), and 1,573 genes (670 downregulated, 903 upregulated) were differentially expressed between *Shh-P1* and control embryos (Fig. 1 A,B, Tables S1, S2). We intersected these datasets to uncover genes that were both downregulated in *Smo*^{ecko} and upregulated in *Shh-P1* (Shh activated genes), or upregulated in *Smo*^{ecko} and downregulated in *Shh-P1* (Shh repressed genes). This comparative transcriptome analysis revealed that Shh signaling is necessary and sufficient for the activation of 141 genes and repression of 77 genes in the otic vesicle at E11.5 (Fig. 1C-F, Fig. S1, Tables S3, S4).

Shh activated genes are significantly enriched in gene ontology (GO) terms associated with inner ear morphogenesis, sensory perception of sound, cochlear development and Hedgehog signaling activity (Fig. 1G). Of the top 50 Shh activated genes, 20 have documented inner ear expression in peer reviewed publications, including seven with established roles in cochlear development and/or auditory function (Fig. 1D). Genes in this category are likely to serve as Shh dependent regulators of cochlear development.

Shh repressed genes are also enriched for GO terms associated with inner ear morphogenesis (Fig. S1 and Table S4). Several of these genes (*Hmx2, Hmx3, Bmp4, Msx1, Msx2, Meis1, Meis2*) are expressed in dorsal regions of the otic vesicle, and/or have known roles in vestibular development (Wang et al., 2004; Chang et al., 2008; Sánchez-Guardado et al., 2011**)**. These results suggest that Shh signaling within the

147 otic epithelium may be required to prevent a subset of dorsal otic genes from being
148 ectopically expressed in ventral regions of the otic vesicle.
149 Not all previously described Shh responsive genes in the inner ear were
150 differentially expressed in both *Smo*^{ecko} and *Shh-P1* embryos. For instance, expression
151 of the homeodomain transcription factor, *Otx2,* was downregulated five-fold in *Smo*^{ecko}
152 mutants, but was unaltered in *Shh-P1* embryos (Tables S1, S2). On the other hand,
153 some genes (e.g. *Six1*, *Eya1* and *Jag1*) that showed no change in mRNA transcript
154 abundance between *Smo*^{ecko} and control littermates were significantly upregulated in
155 *Shh-P1* embryos (Tables S1, S2). Hence, we considered any genes exhibiting loss
156 and/or gain of expression in either *Smo*^{ecko} or *Shh-P1* embryos as candidate *Shh*
157 responsive genes in the otic vesicle.
158 To validate the expression of candidate Shh responsive genes in the developing
159 cochlear duct we selected 24 genes that were downregulated in *Smo*^{ecko} and/or
160 upregulated in *Shh-P1* embryos for further analysis by in situ hybridization. Many of
161 these genes (n=17) have known or predicted roles in cochlear development, including
162 seven (*Emx2*, *Eya1*, *Eya4*, *Mpzl2*, *Pls1*, *Six1*, *Gata3*) that when mutated cause hearing
163 loss in humans and/or mice (https://hereditaryhearingloss.org/recessive-genes;
164 http://www.informatics.jax.org). The expression of seven additional genes (*Dsp,*
165 *Pcdh11x, Brip1, Gas2, Fam107a, Slc39a8, Capn6*) had not previously been described
166 in the otic vesicle.
167 Four genes (*Gli1*, *Pax2*, *Gata3* and *Otx2*), already characterized as Shh
168 dependent transcription factors (Brown and Epstein, 2011), exhibit distinct patterns of
169 expression in the otic vesicle at E11.5 that include broad ventral (*Gli1*), medial wall
170 (*Pax2*), ventral tip (*Gata3*), and lateral wall (*Otx2*) domains (Fig. 2). Remarkably, all
171 other genes selected for follow up analysis were expressed in one of these four Shh
172 responsive regions. For instance, known (*Emx2*, *Eya1* and *Eya4*) and previously
173 uncharacterized (*Dsp, Mpzl2 and Pcdh11x*) genes were broadly expressed in the
174 ventral half of the otic vesicle in a similar pattern with *Gli1* (Fig. 2). Six genes (*Brip1,*
175 *Car13, Gas2, Fam107a, Pls1 and Six1*) displayed overlapping expression with *Pax2* on
176 the medial side of the otic vesicle (Fig. 2). Six other genes (*Ano1, Fst, Hey1, Jag1,*
177 *Lin28b* and *Slc39a8*) were expressed in the ventral tip of the otic vesicle in a similar

pattern to *Gata3*, including genes (*Hey1, Jag1, Lin28b*) implicated in prosensory development (Benito-Gonzalez and Doetzlhofer, 2014; Kiernan and Gridley, 2006; Golden et al., 2015). Finally, two genes (*Capn6, Rspo2*) were expressed on the lateral wall of the otic vesicle, comparable to *Otx2*. These results demonstrate the utility of our differential RNA-seq analysis for discovery of Shh responsive genes expressed in discrete ventral territories of the otic vesicle during the initial stages of cochlear duct outgrowth.

Given that the otic vesicle fails to extend ventrally in Smo^{ecko} embryos at E11.5, the reduced expression of Shh responsive genes may be due to the loss of Shh signaling activity, or to the loss of ventral otic tissue. To discern between these two possibilities, we evaluated expression one day earlier, at E10.5, prior to the emergence of differences in otic vesicle morphology between Smo^{ecko} and control embryos (Fig. 3). Our earlier work revealed that expression of *Gli1*, *Pax2*, *Gata3,* and *Otx2* was absent from Smo^{ecko} otic vesicles at E10.5 (Brown and Epstein, 2011). Similarly, the majority of Shh responsive genes analyzed here showed abrogated otic expression in Smo^{ecko} mutants compared to control littermates at E10.5 (Fig. 3). It should be noted that compared to E11.5, the expression of several of these genes was weaker (*Dsp, Emx2, Mpzl2, Car13, Pls1, Hey1*) or not detected (*Fst, Pcdh11x*) in control embryos at E10.5.

The expression of *Six1* and *Jag1*, with defined roles in prosensory development, displayed more complex alterations in Smo^{ecko} mutants. These genes are prominently expressed on the ventromedial side of the otic vesicle in control embryos (Fig. 3), encompassing prospective sensory progenitors that begin to differentiate after E12.5 (Ruben, 1967; Chen and Segil, 1999). Interestingly, the expression of *Six1* and *Jag1* is flipped in Smo^{ecko} mutants, with loss of medial and gain of lateral otic staining (Fig.3). Two other genes (*Eya1* and *Eya4*) with broad ventral expression in the otic vesicle at E11.5 showed loss of medial and maintenance of lateral otic expression in Smo^{ecko} mutants (Fig. 3). Since Eya1 and Six1 form a transcriptional complex with Sox2 to regulate hair cell development (Ahmed et al., 2012), we evaluated Sox2 expression in Smo^{ecko} mutants, which also exhibited a medial to lateral switch in otic vesicle expression (Fig. S2). Not all genes expressed along the ventromedial wall showed flipped expression in Smo^{ecko} mutants, suggesting that this phenomenon may be

specific for genes with prosensory function. Since Otx2 is required to repress sensory development on the lateral (nonsensory) side of the cochlear duct (Vendrell et al., 2015), we posit that the downregulation of *Otx2* in *Smo^{ecko}* embryos accounts for the derepression of genes with prosensory function on the lateral wall of the otic vesicle.

We also addressed the sufficiency of Shh to activate candidate target genes in the otic vesicle by evaluating their expression in *Shh-P1* embryos. The majority of genes (21/24) were ectopically expressed in broad dorsal (*Emx2, Eya1, Eya4, Mpzl2, Pcdh11x, Pax2, Pls1*) or lateral (*Dsp, Brip1, Car13, Gas2, Fam107a, Six1, Gata3, Ano1, Fst, Hey1, Jag1, Lin28b, Slc39a8*) regions of the otic vesicle in *Shh-P1* embryos at E11.5 (Fig. 4). Three genes (*Otx2, Capn6, Rspo2*) expressed in a ventrolateral otic domain did not show ectopic expression in *Shh-P1* embryos, suggesting that additional factors are required for their activation in conjunction with Shh. Taken together, these data identify a set of Shh responsive genes with known and potentially novel roles in early aspects of cochlear development.

ATAC-seq identifies active regulatory sequences in the otic vesicle

The expression of Shh responsive genes in the inner ear may be directly regulated by Gli2 and Gli3 (Bok et al., 2007), indirectly regulated by other Shh dependent transcription factors (e.g. *Pax2, Gata3, Otx2*), or by a combination of Shh dependent and independent transcription factors, as described in the spinal cord (Peterson et al., 2012; Oosterveen et al., 2012). As an entry point to deciphering the transcriptional mechanisms regulating Shh target gene expression in the inner ear, we performed ATAC-seq on chromatin isolated from wild type otic vesicles at E11.5. ATAC-seq profiles from four highly correlated biological replicates (peaks present in at least two samples) were merged, yielding 30,720 regions of open chromatin accessibility that map to intergenic (22.7%), intronic (24.3%), exonic (5.3%) and promoter (47.6%) regions of the genome (Fig. 5A).

Gene regulatory sequences typically reside within regions of open chromatin (Buenrostro et al., 2013; Vierstra and Stamatoyannopoulos, 2016). In agreement with this observation, promoters of actively transcribed genes in the inner ear (RNA-seq, RPKM≥1) were more likely to display ATAC-seq signal compared to promoters of

inactive genes (RNAseq, RPKM<1) (Fig. 5B). ATAC-seq peaks were also selectively enriched on functionally validated mouse inner ear enhancers (80%) from the VISTA Enhancer Database (Visel et al 2007), compared to hindbrain (22%) and limb (21%) enhancers (Fig. 5C,D,F). Similar ATAC-seq signal enrichment was observed for orthologous mouse sequence of human inner ear enhancers (32%) compared to hindbrain (10%) and limb (8.5%) enhancers, although levels are overall lower than for mouse enhancers (Fig. 5C,E,G).

Non-coding ATAC-seq peaks were also enriched in the vicinity of genes annotated for terms associated with inner ear gene expression and mouse phenotypes according to the GREAT analysis tool (Fig. S3; Mclean et al., 2010). Moreover, non-coding ATAC-seq peaks from the inner ear were specifically more conserved within placental mammals, as opposed to across more distantly related vertebrates, compared to other tissues, suggesting that evolutionary changes in gene regulatory sequences may underlie mammalian specific adaptations in inner ear morphology (Fig. 5H). Taken together, these findings suggest that the inner ear ATAC-seq dataset represents a robust resource for identifying functional regulatory sequences controlling gene expression in the developing otic vesicle.

Discovery of Shh dependent inner ear enhancers through genomic integration

To identify Shh dependent regulatory sequences in the inner ear, we overlaid ATAC-seq and Gli2 ChIP-seq datasets (Fig. 6A). Unfortunately, it was not feasible to perform Gli2 ChIP-seq on isolated otic vesicles due to technical limitations with small scale tissue samples. Nevertheless, we took advantage of a Gli2 ChIP-seq dataset using embryonic mouse heads at E10.5, which included the otic vesicles (see methods). We found that 4% (605/14457) of intergenic and intronic ATAC-seq peaks overlapped with Gli2 occupied sites (Fig. 6B). Notably, gene set enrichment analysis demonstrated that Shh activated genes are significantly enriched around regions of open chromatin co-bound by Gli2 (FDR≤0.05), consistent with the premise that expression of these genes is directly regulated by Shh/Gli2 (Fig. 6C). Approximately, 20% (137/605) of overlapping ATAC-seq/Gli2 ChIP-seq sites also intersected with H3K27ac ChIP-seq peaks from E11.5 hindbrain (ENCODE project, ENCSR129LAP), a histone modification

commonly associated with active enhancers (Fig. 6B). However, Shh activated genes were not enriched around overlapping genomic sites for these three signals, suggesting that the H3K27ac ChIP-seq dataset from hindbrain may not be a good predictor of Shh/Gli2 dependent enhancers in the inner ear (Fig. S4).

We next analyzed the DNA sequence at overlapping ATAC-seq/Gli2 ChIP-seq genomic regions for enrichment of motifs matching transcription factor binding sites (TFBS). As expected, the most over-represented motif matched the consensus binding sequence for Gli proteins (Fig. 6D). Other significantly enriched motifs included binding sites for CTCF, Sox2, Six and Tead family members. The presence of Sox2 and Six binding sites is particularly intriguing given that the activity of enhancers controlling expression of Shh/Gli target genes in the neural tube is often dependent on Sox2 (Peterson et al., 2012; Oosterveen et al., 2012), and both Sox2 and Six1 are essential for inner ear development (Zheng et al., 2003; Ozaki et al., 2004; Kiernan et al., 2005; Stevens et al., 2019).

Six1$^{-/-}$ and *Smo*^{ecko} embryos display similar defects in cochlear duct outgrowth and misexpress several of the same genes in the otic vesicle (Ozaki et al., 2004; Brown and Epstein, 2011). Some of the phenotypic overlap between *Six1*$^{-/-}$ and *Smo*^{ecko} may be attributed to altered *Six1* expression in *Smo*^{ecko} embryos (Fig. 3). A reciprocal downregulation in Shh signaling was not observed in *Six1*$^{-/-}$ mutant ears (Ozaki et al., 2004). It is also feasible that Gli2 and Six1 converge on common enhancers to co-regulate target gene expression. To address this possibility, we performed ChIP-qPCR on chromatin isolated from otic vesicles at E11.5 using antibodies against Gli2 and Six1. Putative inner ear enhancers (IEEs) with Gli and Six binding sites in the vicinity of Shh responsive genes (*Frem1*, *Ecel1*, *Fam107a*, *Hey1*, *Cldn22*) demonstrated significant co-occupancy of Gli2 and Six1, with the exception of *Ecel1*, which did not show Gli2 enrichment (Fig. 6E,F). These results suggest that a subset of Shh responsive genes in the inner ear may be co-regulated by Gli2 and Six1.

***In vivo* validation of candidate inner ear enhancers**

Three candidate IEEs were selected for functional validation in a transgenic mouse reporter assay based on the presence of an ATAC-seq signal, conservation of at

least one Gli binding site, and proximity to a Shh responsive gene (Fig. 7A,C,E). Candidate IEEs located in introns of *Jag1*, *Pls1* and *Brip1* demonstrated significant Gli2 enrichment, as assessed by ChIP-qPCR using chromatin isolated from otic vesicles at E11.5 (Fig. 7G). Results for Gli2 and H3K27ac occupancy at IEEs were more variable in ChIP-seq datasets from whole brain and hindbrain, respectively, possibly due to under-representation of inner ear tissue in these samples (Fig. 7A,C,E). Remarkably, each of the three IEEs generated reproducible patterns of X-gal staining in the otic vesicle of transgenic embryos, recapitulating aspects of endogenous gene expression (Fig. 7B,D,F and Table 1). ATAC-seq peaks in the vicinity of two other Shh responsive genes (*Gas2* and *Fam107a*) that did not contain Gli binding sites failed to activate reporter expression in transgenic embryos (Table 1). These results suggest that chromatin accessibility on its own may not be sufficient to accurately predict genomic regions with tissue specific enhancer activity in the inner ear. In sum, our integrated genomic approach successfully identified Shh dependent genes and enhancers in the inner ear that should assist future studies designed to address the functional impact of these factors on cochlear duct outgrowth.

DISCUSSION

Classification of Shh responsive genes during inner ear development

We exploited *Smo*^{ecko} and *Shh-P1* mutant embryos to identify a comprehensive set of differentially expressed genes in the inner ear that are transcriptionally activated and repressed by Shh signaling during the initial stages of cochlear duct outgrowth at E11.5. Many of these differentially expressed genes have well defined roles in cochlear development and/or auditory function but were not previously known to be dependent on Shh for their expression. Our analysis also uncovered genes with previously uncharacterized inner ear expression that represent strong candidates for follow up studies to investigate their roles in cochlear morphogenesis.

A novel outcome of this work is the observation that Shh responsive genes are partitioned into four expression domains in the ventral half of the otic vesicle. This finding reveals several new insights into the role of Shh in assigning regional and cellular identities to otic epithelial progenitors. Firstly, the 'broad ventral' class of Shh responsive genes distinguishes auditory (ventral) from vestibular (dorsal) regions of the otic vesicle (Fig. 2). Secondly, the downregulation of genes (e.g. *Eya1*, *Six1*, *Jag1* and *Sox2*) with essential roles in prosensory development in 'broad ventral', 'medial wall' and 'ventral tip' regions of the otic vesicle in *Smo*^{ecko} embryos highlights a previously unappreciated role for *Shh* in regulating transcription of genes that prime the medial wall of the cochlear duct for subsequent sensory development. Thirdly, loss of *Otx2* expression on the ventrolateral side of *Smo*^{ecko} otic vesicles likely explains the ectopic expression of prosensory markers, indicating an additional role for Shh in ensuring correct positioning of the prosensory domain. Since conditional *Otx2* mutants also show ectopic expression of prosensory markers in non-sensory regions of the cochlear duct (Vendrell et al., 2015), and that *Mycn* and *Six1* mutants display similar phenotypes, including the downregulation of *Otx2* expression (Ozaki et al., 2004; Vendrell et al., 2015), we propose that Shh/Gli, Mycn and Six1 cooperate to regulate *Otx2* expression on the ventrolateral side of the otic vesicle.

Prior studies demonstrated requirements for Shh in limiting the size of the prosensory domain and preventing precocious cell cycle exit and/or differentiation of

sensory progenitors (Driver et al., 2008; Bok et al., 2013). These functions contrast with those described in our study in that they are mediated by a different source of Shh (spiral ganglia versus notochord) acting at a later stage of development (E13.5 versus E10.5). Thus, Shh signaling fulfills spatially and temporally distinct roles in regulating positive and negative aspects of sensory epithelia formation in the cochlear duct.

Characterization of inner ear enhancers regulating Shh responsive genes

The overlap in expression of Shh responsive genes with transcription factors (*Gli1*, *Pax2*, *Gata3*, *Otx2*) in each of the four Shh responsive regions of the otic vesicle suggested a possible mode of regulation. In partial support of this claim, we observed an enrichment of Shh responsive genes in the vicinity of putative IEEs identified by sites of chromatin accessibility and Gli2 occupancy. Gli motifs were the most abundant TFBS in these putative IEEs, whereas, binding sites for other Shh dependent transcription factors (Pax2, Gata3, Otx2) were not enriched in this dataset. These results suggest that Pax2, Gata3 and Otx2 may not play a significant role in the direct regulation of Shh responsive genes at E11.5, but leaves open the possibility that they may do so at earlier stages of inner ear development.

Despite the absence of predicted TFBS from putative Shh dependent IEEs, our analysis identified other transcription factors, including Six1 and Sox2, that may cooperate with Gli2 in the direct regulation of Shh responsive genes in the otic vesicle at E11.5. Six1 is a particularly compelling candidate given the phenotypic similarities between *Six1*$^{-/-}$ and *Smo*^{ecko} mutants, including cochlear agenesis and altered dorsoventral patterning of the otic vesicle, suggesting that Gli2 and Six1 may regulate common target genes (Zheng et al., 2003; Ozaki et al., 2004; Brown and Epstein, 2011). The co-recruitment of Gli2 and Six1 to a subset of putative IEEs in the vicinity of Shh responsive genes is consistent with this premise.

We also demonstrated that sites of open chromatin overlapping with conserved Gli binding sites in the vicinity of Shh responsive genes are good predictors of functional IEEs. Interestingly, IEEs with optimal (*Jag1*) and low to moderate (*Pls1, Brip1*) affinity Gli motifs each directed patterns of reporter activity in the ventral otocyst that resembled expression of the nearby gene. Thus, unlike Hh/Gli signaling in other developmental

contexts, Gli binding site quality does not appear to correlate with enhancer activity in Shh responsive cells in the inner ear (Peterson et al., 2012; White et al., 2012; Ramos and Barolo 2013; Lorberbaum et al., 2016).

The three genes (*Jag1*, *Pls1* and *Brip1*) for which IEEs were identified were not previously known to be regulated by Shh signaling. Gain and loss of function studies indicate that Jag1, a Notch ligand, is required for prosensory development (Kiernan et al., 2001; Kiernan et al., 2005; Kiernan et al., 2006; Brooker et al., 2006). The initiation of *Jag1* expression in the otic placode is regulated by Wnt signaling (Jayasena et al., 2008), whereas our data suggests that maintenance of *Jag1* in prosensory progenitors is dependent on Shh. Pls1 is an actin bundling protein that maintains the length and width of stereocilia in inner hair cells and is required for optimal hearing in adult mice (Taylor et al., 2015). Since Pls1 is dispensable for the initial formation of stereocilia, it remains to be determined what role its Shh regulated expression might play during otic development. Similarly, the inner ear function of Brip1, a member of the RecQ DEAH helicase family that interacts with Brca1 in DNA damage repair and tumor suppression, is currently unknown (Ouhtit et al., 2016).

In summary, our integrated genomic approach greatly expands the list of genes and regulatory sequences that depend on Shh signaling in the inner ear. These datasets should benefit future studies addressing the function and regulation of key genes acting downstream of Shh that promote cochlear duct morphogenesis and establish its distinct cellular composition.

MATERIALS AND METHODS

Mouse Lines

All mouse experiments were performed in accordance with the ethical guidelines of the National Institutes of Health and with the approval of the Institutional Animal Care and Use Committee of the University of Pennsylvania. The production of *Smo*^{ecko} (*Foxg1cre; Smo*$^{loxp/-}$) and control (*Foxg1cre; Smo*$^{loxp/+}$) embryos was described previously (Brown and Epstein, 2011). The *Shh-P1* mouse line was described previously (Riccomagno et al., 2002).

RNA-seq analysis

Otic vesicles from control, *Smo*^{ecko} and *Shh-P1* embryos (n=4 pairs of biological replicates for each genotype) were isolated at E11.5, exposed to collagenase P (1mg/ml) at 37^{o}C for 20 min to remove surrounding mesenchyme, and submerged in RNA*later*™ Stabilization Solution (Thermo Fisher Scientific, Cat#AM7022). RNA was extracted using the RNeasy Micro Kit (Qiagen, Cat#74004). Total RNA (200ng) was used for poly A selected RNA-seq library preparation using the NEBNext® Ultra™ Directional RNA Library Prep Kit for Illumina® (mRNA) (New England Biolabs Cat#E7530S). Biological replicates were individually barcoded, pooled, and sequenced to generate 100bp single-end reads on one lane of a HiSeq4000 instrument at the Next Generation Sequencing Core (Perelman School of Medicine, University of Pennsylvania). RNA-seq reads were aligned to the mm9 mouse genome build (http://genome.ucsc.edu/) using RUM (Grant et al. 2011). Differential gene expression analysis between *Smo*^{ecko}, *Shh-P1* and control samples was performed using edgeR (Robinson et al., 2010). Heatmaps for RNA-seq data were generated using PIVOT (Zhu et al., 2018). RNA-seq data were deposited in NCBI GEO under accession number GSE131165.

ATAC-seq analysis

Four independent ATAC-seq libraries were generated from wild type otic vesicles **(**n=10 per library**)** isolated at E11.5 using 50,000 cells per replicate as described (Buenrostro

et al., 2015). Tagmentation was performed using the Nextera® DNA Library Preparation Kit (Illumina® 15028211). Multiplexed 50 bp paired-end sequence reads were generated on a single lane of an Illumina HiSeq2000 instrument. ATAC-seq reads were mapped to the mm9 mouse genome build (http://genome.ucsc.edu/) using Bowtie with default parameters (Langmead et al., 2009). Regions of open chromatin were identified by MACS2 using default parameters (Zhang et al., 2008). Only high confidence peaks that were present in at least two libraries were reported. ATAC-seq data were deposited in NCBI GEO under accession number GSE131165.

Gli2 ChIP-seq

Mouse embryonic tissues were harvested from timed matings between Swiss Webster (Taconic) mice where day of detection of vaginal plug was considered embryonic day E0.5. ChIP was performed on pooled tissue obtained from 40 E10.5 heads isolated below the otic vesicle and processed for ChIP as described (Peterson et al., 2012). Briefly, embryonic tissue was fixed for 30 minutes in 1% formaldehyde/PBS at room temperature followed by quenching with 125 mM glycine. ChIP was performed on the entire lysate using magnetic Dynabeads™ Protein G (Thermo Fisher Scientific) bound with goat anti-Gli2 antibody (R&D Cat# AF3635). A ChIP DNA library was prepared for Illumina Sequencing according to manufacturer recommendations and 50 bp single-end reads were obtained from a Hi-Seq2000 instrument. The resulting reads were mapped to mouse genome assembly mm9 (http://genome.ucsc.edu/) using Bowtie (Langmead et al., 2009). Gli2 ChIP-seq data were deposited in NCBI GEO under accession number GSE131165.

Intersection of ATAC-seq and Gli2 ChIP-seq data

Enriched peaks from the ATAC-seq and Gli2 ChIP-seq were intersected using Bedtools intersect interval function (Galaxy Version 2.27.1+galaxy1) with the parameter, *-wa, overlap on either strand* and returning full length ATAC-seq peaks that overlap with Gli2 ChIP-seq peaks (Quinlan and Hall, 2010).

463 ***ATAC-seq enrichment at inner ear promoters and VISTA enhancers***

464 ATAC-seq promoter peaks were first identified by intersecting RefSeq (mm9) genes
465 extracted from UCSC Genome Browser (Table Browser; parameter: create one Bed
466 record per upstream by 500 bp) using Bedtools intersect interval function (Galaxy
467 Version 2.27.1+galaxy1) with the parameter, *-wa, overlap on either strand* and returning
468 RefSeq peaks. The gene name was then used to compare against E11.5 control RNA-
469 seq genes that are expressed (RPKM≥1.0) or not expressed (RPKM<1.0) in the otic
470 vesicle. The enrichment of ATAC-seq peaks against VISTA enhancers
471 (https://enhancer.lbl.gov/) was performed by converting enhancer coordinates to peak
472 files and then intersected with ATAC-seq non-coding peaks using Bedtools (parameters
473 similar to above and returning ATAC-seq peaks).
474
475 ***ATAC-seq conservation analysis***

476 We measured placental mammal-derived (PS) and vertebrate-derived (VS) PhyloP
477 scores within each ATAC-seq peak, and estimated the ratio of these values for each
478 tissue. For each tissue, we first identified the mode of the enhancer peak width
479 distribution, so that each called peak could be elongated or trimmed to a standard peak
480 size. Then, extending peaks shorter than this mode, or contracting peaks longer than
481 the mode, we estimated PS and VS for each base of each peak. For each tissue, the
482 mean PS and VS were higher at the center of the peak compared to the edges. Since
483 the PS and VS have different ranges of values, we used their ratio for comparison
484 between tissues instead of using their absolute values. For each base position, we then
485 obtained the ratio of the mean PS score to the mean VS score across all peaks in that
486 tissue. As a control, we also took the set of all exons in the mouse genome, and
487 defining a peak of length 201, obtained PS and VS for each base of each exon.
488
489 ***Functional annotation analysis of ATAC-seq data***

490 Functional annotation analysis of ATAC-seq data was performed using GREAT version
491 3.0.0 (McLean et al., 2010), linking peaks to the nearest transcription start site
492 (TSS) ± 100 kb. Functional terms were selected based on reported significance score
493 and relevance to the biological system.

494 ***Gene set enrichment analysis (GSEA)***

495 GSEA was performed using the GSEA software (MSigDB 6.1 and 6.2) as described
496 (Mootha et al., 2003; Subramanian et al., 2005). Ranked file (rnk) for Shh activated
497 genes was prepared from the RNA-seq differential expression analyses based on the
498 $\log_2$ fold change. The .grp files were prepared from expressed genes (i.e. RNA-seq,
499 RPKM ≥ 1.0) that are found within the intersected peaks: i) ATAC-seq and Gli2 ChIP-
500 seq ± 500 kb (Fig. 6C) and ii) ATAC-seq, Gli2 ChIP-seq and H3K27ac ChIP-seq peaks
501 ± 500 kb (Fig. S4).
502
503 ***ChIP-qPCR***
504 Otic vesicles were dissected in DMEM (with 10% fetal bovine serum) from
505 approximately 25-30 E11.5 embryos per replicate pool (n=3 replicates), homogenized
506 into small pieces, and crosslinked with 1% paraformaldehyde for 15 min at room
507 temperature with shaking. ChIP was performed essentially as described on three
508 biological replicates (Zhao et al., 2012) using 6 µg of anti-Gli2 (R&D Cat# AF3635), anti-
509 Six1 (Cell Signaling Technology, Cat#12891) or anti-immunoglobulin G (IgG) (Cell
510 Signaling Technology) antibodies. QPCR was conducted as described (Zhao et al.,
511 2012) using primer sequences listed in Table S5. Positive control primers in Fig. 7G
512 amplify a DNA fragment from a *Ptch1* enhancer bound by Gli2.
513
514 ***Transgenic mouse reporter assay***
515 Candidate inner ear enhancers were cloned into a vector containing the *Hsp68*
516 promoter, *lacZ* gene and SV40 poly(A) cassette. Transient transgenic embryos were
517 generated by pronuclear injection into fertilized mouse eggs derived from the (BL6xSJL)
518 F1 mouse strain (Jackson Laboratories) at the Transgenic and Chimeric Mouse Facility
519 (Perelman School of Medicine, University of Pennsylvania). For X-gal staining, embryos
520 were harvested at E11.5, fixed in 0.2% glutaraldehyde/1% formaldehyde at 4°C for 30
521 minutes, and stained in a solution containing 1 mg/ml X-gal at 37°C for two hours to
522 overnight.
523
524

Statistical analysis

Relevant information for each experiment including n-values, statistical tests and reported p-values are found in the legend corresponding to each figure. In all cases $p \leq 0.05$ is considered statistically significant and error bars represent standard error of the mean.

Data availability

RNA-seq, ATAC-seq and ChIP-seq datasets have been deposited in NCBI under GEO accession number GSE131165.

Acknowledgements

We thank Dr. Jean Richa and his staff at the Transgenic and Chimeric Mouse Facility (Perelman School of Medicine, University of Pennsylvania) for their assistance in transgenic mouse production, as well as Dr. Jonathan Schug and his team at PSOM NGSC for sequencing services. We also thank members of the Epstein lab for critical comments on this study.

Competing Interests

No competing interests declared.

Author contributions

V.M., A.M.R., S.M.R., Y.Y., A.S.B., and K.A.P performed the experiments. Y-T.Z., J.M., K-J.W., S.R., C.D.B. and V.M. performed data analysis, V.M., Y.Y. and D.J.E. conceived the project. V.M. and D.J.E. wrote the manuscript.

Funding

This work was supported by a grant from the National Institutes of Health [R01 DC006254] to D.J.E.

REFERENCES

Bai, C.B., Stephen, D. and Joyner, A.L. (2004). All mouse ventral spinal cord patterning by hedgehog is Gli dependent and involves an activator function of Gli3. *Dev Cell.* **6**, 103-15.

Basch, M.L., Brown, R.M. 2nd, Jen, H.I. and Groves, A.K. (2016). Where hearing starts: the development of the mammalian cochlea. *J Anat.* **228,** 233-54.

Benito-Gonzalez, A. and Doetzlhofer, A. (2014). Hey1 and Hey2 control the spatial and temporal pattern of mammalian auditory hair cell differentiation downstream of Hedgehog signaling. *J Neurosci.* **34,**12865-76.

Bok, J., Dolson, D. K., Hill, P., Ruther, U., Epstein, D. J. and Wu, D. K. (2007). Opposing gradients of Gli repressor and activators mediate Shh signaling along the dorsoventral axis of the inner ear. *Development* **134,** 1713-22.

Bok, J., Zenczak, C., Hwang, C.H. and Wu, D.K. (2013). Auditory ganglion source of Sonic hedgehog regulates timing of cell cycle exit and differentiation of mammalian cochlear hair cells. *Proc Natl Acad Sci U S A.* **110,** 13869-74.

Brooker, R., Hozumi, K. and Lewis, J. (2006). Notch ligands with contrasting functions: Jagged1 and Delta1 in the mouse inner ear. *Development* **133,** 1277-86.

Brown, A.S. and Epstein, D.J. (2011). Otic ablation of Smoothened reveals direct and indirect requirements for Hedgehog signaling in inner ear development. *Development* **138,** 3967-3976.

Buenrostro, J.D., Giresi, P.G., Zaba, L.C., Chang, H.Y. and Greenleaf, W.J. (2013). Transposition of native chromatin for fast and sensitive epigenomic profiling of open chromatin, DNA-binding proteins and nucleosome position. *Nat Methods*. **10,** 1213-8.

Chang, W., Lin, Z., Kulessa, H., Hebert, J., Hogan, B.L. and Wu, D.K. (2008). Bmp4 is essential for the formation of the vestibular apparatus that detects angular head movements. *PLoS Genet.* **4,** e1000050.

Chen, P. and Segil, N. (1999). p27(Kip1) links cell proliferation to morphogenesis in the developing organ of Corti. *Development* **126,** 1581-90.

Driver, E.C., Pryor, S.P., Hill, P., Turner, J., Rüther, U., Biesecker, L.G., Griffith, A.J. and Kelley, M.W. (2008). Hedgehog signaling regulates sensory cell formation and auditory function in mice and humans. *J Neurosci*. **28,** 7350-8.

Dror, A.A. and Avraham, K.B. (2010). Hearing impairment: a panoply of genes and functions. *Neuron* **68,** 293–308.

Falkenstein, K.N. and Vokes, S.A. (2014). Transcriptional regulation of graded Hedgehog signaling. *Semin Cell Dev Biol.* **33,** 73-80.

Fettiplace, R. (2017). Hair Cell Transduction, Tuning, and Synaptic Transmission in the Mammalian Cochlea. *Compr. Physiol.* **7,** 1197–1227.

Grant, G.R., Farkas, M.H., Pizarro, A.D., Lahens, N.F., Schug, J., Brunk, B.P., Stoeckert, C.J., Hogenesch, J.B., and Pierce, E.A. (2011). Comparative analysis of RNA-Seq alignment algorithms and the RNA-Seq unified mapper (RUM). *Bioinformatics* **27***,* 2518–2528.

Golden, E.J., Benito-Gonzalez, A., Doetzlhofer, A. (2015). The RNA-binding protein LIN28B regulates developmental timing in the mammalian cochlea. *Proc Natl Acad Sci U S A*. **112,** E3864-73.

Jackler, R.K., Luxford, W.M. and House, W.F. (1987). Congenital malformations of the inner ear: a classification based on embryogenesis. *Laryngoscope* **97,** 2-14.

Jayasena, C.S., Ohyama, T., Segil, N. and Groves, A.K. (2008). Notch signaling augments the canonical Wnt pathway to specify the size of the otic placode. *Development* **135,** 2251-61.

Kazmierczak, P., and Müller, U. (2012). Sensing sound: molecules that orchestrate mechanotransduction by hair cells. *Trends Neurosci*. **35,** 220–229.

Kiernan, A.E., Ahituv, N., Fuchs, H., Balling, R., Avraham, K.B., Steel, K.P., and Hrabé de Angelis, M. (2001). The Notch ligand Jagged1 is required for inner ear sensory development. *Proc Natl Acad Sci U S A*. **98,** 3873-8.

Kiernan, A.E., Pelling, A.L., Leung, K.K., Tang, A.S., Bell, D.M., Tease, C., Lovell-Badge, R., Steel, K.P. and Cheah, K.S. (2005). Sox2 is required for sensory organ development in the mammalian inner ear. *Nature* **434,** 1031-5.

Kiernan, A.E., Xu, J. and Gridley, T. (2006). The Notch ligand JAG1 is required for sensory progenitor development in the mammalian inner ear. *PLoS Genet*. **2,** e4.

Korver, A.M., Smith, R.J., Van Camp, G., Schleiss, M.R., Bitner-Glindzicz, M.A., Lustig, L.R., Usami, S.I. and Boudewyns, A.N. (2017). Congenital hearing loss. *Nat Rev Dis Primers* **3,** 16094.

Langmead, B., Trapnell, C., Pop, M. and Salzberg, S.L. (2009). Ultrafast and memory-efficient alignment of short DNA sequences to the human genome. *Genome Biol.* **10,** R25.

Lorberbaum, D.S., Ramos, A.I., Peterson, K.A., Carpenter, B.S., Parker, D.S., De, S., Hillers, L.E., Blake, V.M., Nishi, Y., McFarlane, M.R., Chiang, A.C., Kassis, J.A.,

Allen, B.L. and McMahon, A.P. and Barolo, S. (2016). An ancient yet flexible cis-regulatory architecture allows localized Hedgehog tuning by patched/Ptch1. *Elife.* **5,** e13550.

McLean, C.Y., Bristor, D., Hiller, M., Clarke, S.L., Schaar, B.T., Lowe, C.B., Wenger, A.M. and Bejerano, G. (2010). GREAT improves functional interpretation of cis-regulatory regions. *Nat Biotechnol.* **28,** 495-501.

Montcouquiol, M. and Kelley, M.W. (2019). Development and Patterning of the Cochlea: From Convergent Extension to Planar Polarity. *Cold Spring Harb Perspect Med.* Jan 7. pii: a033266.

Mootha, V.K., Lindgren, C.M., Eriksson, K.F., Subramanian, A., Sihag, S., et al. (2003). PGC-1alpha-responsive genes involved in oxidative phosphorylation are coordinately downregulated in human diabetes. *Nat Genet.* **34,** 267-73.

Oosterveen, T., Kurdija, S., Alekseenko, Z., Uhde, C.W., Bergsland, M., Sandberg, M., Andersson, E., Dias, J.M., Muhr, J. and Ericson, J. (2012). Mechanistic differences in the transcriptional interpretation of local and long-range Shh morphogen signaling. *Dev Cell.* **23,**1006-19.

Oosterveen, T., Kurdija, S., Ensterö, M., Uhde, C.W., Bergsland, M., Sandberg, M., Sandberg, R., Muhr, J. and Ericson, J. (2013). SoxB1-driven transcriptional network underlies neural-specific interpretation of morphogen signals. *Proc Natl Acad Sci U S A.* **110,** 7330-5.

Ouhtit, A., Gupta, I. and Shaikh, Z. (2016). BRIP1, a potential candidate gene in development of non-BRCA1/2 breast cancer. *Front Biosci* **8,** 289-98.

Ozaki, H., Nakamura, K., Funahashi, J., Ikeda, K., Yamada, G., Tokano, H., Okamura, H.O., Kitamura, K., Muto, S., Kotaki, H., Sudo, K., Horai, R., Iwakura, Y. and Kawakami, K. (2004). Six1 controls patterning of the mouse otic vesicle. *Development* **131,** 551-62.

Peterson, K.A., Nishi, Y., Ma, W., Vedenko, A., Shokri, L., Zhang, X., McFarlane, M., Baizabal, J.M., Junker, J.P., van Oudenaarden, A., Mikkelsen, T., Bernstein, B.E., Bailey, T.L., Bulyk, M.L., Wong, W.H. and McMahon, A.P. (2012). Neural-specific Sox2 input and differential Gli-binding affinity provide context and positional information in Shh-directed neural patterning. *Genes Dev.* **26,** 2802-16.

Quinlan, A.R. and Hall, I.M. (2010). BEDTools: a flexible suite of utilities for comparing genomic features. *Bioinformatics.* **26,** 841-2.

Ramos, A.I. and Barolo, S. (2013). Low-affinity transcription factor binding sites shape morphogen responses and enhancer evolution. *Philos Trans R Soc Lond B Biol Sci*. **368,** 20130018.

Riccomagno, M. M., Martinu, L., Mulheisen, M., Wu, D. K. and Epstein, D. J. (2002). Specification of the mammalian cochlea is dependent on Sonic hedgehog. *Genes Dev* **16,** 2365-78.

Robinson, M.D., McCarthy, D.J., and Smyth, G.K. (2010). edgeR: a Bioconductor package for differential expression analysis of digital gene expression data. *Bioinformatics*. **26,** 139–140.

Ruben, R.J. (1967). Development of the inner ear of the mouse: a radioautographic study of terminal mitoses. *Acta Otolaryngol*. **220,** 1-44.

Sánchez-Guardado, L.Ó., Ferran, J.L., Rodríguez-Gallardo, L., Puelles, L., Hidalgo-Sánchez, M. (2011). Meis gene expression patterns in the developing chicken inner ear. *J Comp Neurol.* **519,** 125-47.

Schwander, M., Kachar, B., and Müller, U. (2010). Review series: The cell biology of hearing. *J. Cell Biol.* **190,** 9–20.

Steevens, A.R., Glatzer, J.C., Kellogg, C.C., Low, W.C., Santi, P.A. and Kiernan, A.E. (2019). SOX2 is required for inner ear growth and cochlear nonsensory formation prior to sensory development. *Development*. May 31. pii: dev.170522. doi: 10.1242/dev.170522. [Epub ahead of print]

Subramanian, A., Tamayo, P., Mootha, V.K., Mukherjee, S., Ebert, B.L., Gillette, M.A., Paulovich, A., Pomeroy, S.L., Golub, T.R., Lander, E.S. and Mesirov, J.P. (2005). Gene set enrichment analysis: a knowledge-based approach for interpreting genome-wide expression profiles. *Proc Natl Acad Sci U S A.* **102,** 15545-50.

Taylor, R., Bullen, A., Johnson, S.L., Grimm-Günter, E.M., Rivero, F., Marcotti, W., Forge, A. and Daudet, N. (2015). Absence of plastin 1 causes abnormal maintenance of hair cell stereocilia and a moderate form of hearing loss in mice. *Hum Mol Genet*. **24,** 37-49.

Vendrell, V., López-Hernández, I., Durán Alonso, M.B., Feijoo-Redondo, A., Abello, G., Gálvez, H., Giráldez, F., Lamonerie, T. and Schimmang, T. (2015). Otx2 is a target of N-myc and acts as a suppressor of sensory development in the mammalian cochlea. *Development* **142,** 2792-800.

Vierstra, J. and Stamatoyannopoulos, J.A. (2016). Genomic footprinting. *Nat Methods*. **13,** 213-21.

Visel, A., Minovitsky, S., Dubchak, I. and Pennacchio, L.A. (2007). VISTA Enhancer Browser--a database of tissue-specific human enhancers. *Nucleic Acids Res*. 35, D88-92.

Wang, W., Grimmer, J.F., Van De Water, T.R. and Lufkin, T. (2004). Hmx2 and Hmx3 homeobox genes direct development of the murine inner ear and hypothalamus and can be functionally replaced by Drosophila Hmx. *Dev Cell*. **7,** 439-53.

White, M.A., Parker, D.S., Barolo, S. and Cohen, B.A. (2012). A model of spatially restricted transcription in opposing gradients of activators and repressors. *Mol Syst Biol*. **8,** 614.

Wu, D.K. and Kelley, M.W. (2012). Molecular mechanisms of inner ear development. *Cold Spring Harb Perspect Biol.* **1,** a008409.

Yu, W.-M., and Goodrich, L.V. (2014). Morphological and physiological development of auditory synapses. *Hear. Res*. **311,** 3–16.

Zhang, Y., Liu, T., Meyer, C.A., Eeckhoute, J., Johnson, D.S., Bernstein, B.E., Nusbaum, C., Myers, R.M., Brown, M., Li, W., Liu, X.S. (2008). Model-based analysis of ChIP-Seq (MACS). *Genome Biol.* **9,** R137.

Zhao, L., Zevallos, S.E., Rizzoti, K., Jeong, Y., Lovell-Badge, R. and Epstein, D.J. (2012). Disruption of SoxB1-dependent Sonic hedgehog expression in the hypothalamus causes septo-optic dysplasia. *Dev Cell*. **22,** 585-96.

Zheng, W., Huang, L., Wei, Z.B., Silvius, D., Tang, B. and Xu, P.X. (2003). The role of Six1 in mammalian auditory system development. *Development* **130,** 3989-4000.

Zhu, Q., Fisher, S.A., Dueck, H., Middleton, S., Khaladkar, M. and Kim, J. (2018). PIVOT: platform for interactive analysis and visualization of transcriptomics data. *BMC Bioinformatics*.**19,** 6.

552 **FIGURE LEGENDS**

553

554 **Figure 1. Differential expression profiling identifies Shh responsive genes in the**
555 **inner ear.** (A, B) Heat maps of differential RNA-seq profiles (log_2 fold change) between
556 (A) control and *Smo*^{ecko} (n=4), and (B) control (n=3) and *Shh-P1* (n=4) inner ears at
557 E11.5 (FDR≤0.05 and RPKM≥1.0). (C) Intersection of differentially expressed genes in
558 *Smo*^{ecko} (red) and *Shh-P1* (blue) inner ears identifies Shh activated (top) and Shh
559 repressed (bottom) gene sets. (D) Top 50 Shh activated genes that show significant
560 downregulation in *Smo*^{ecko} (red) and upregulation in *Shh-P1* (blue) inner ears (log_2 fold
561 change). (E, F) Normalized RNA-seq read counts in *Smo*^{ecko} (red) and *Shh-P1* (blue)
562 mutants of two representative Shh activated genes, *Gli1* and *Fst*. (G) DAVID Gene
563 Ontology term enrichment (Biological Processes) for gene sets that are downregulated
564 in *Smo*^{ecko} (red) and upregulated in *Shh-P1* (blue) mutants.

565

566 **Figure 2. Classification of Shh responsive genes in wild type otic vesicles at**
567 **E11.5.** Schematic of a transverse section through the inner ear color coded to represent
568 the four patterns of Shh responsive genes in broad ventral (magenta diagonal lines) ,
569 medial wall (light blue), ventral tip (dark blue), and lateral wall (green) regions of the otic
570 vesicle. Expression of Shh responsive genes as determined by in situ hybridization on
571 wild type sections through the inner ear at E11.5 (n=3 replicates). Scale bar: 100 μm.
572 Abbreviations: nt, neural tube; D, Dorsal; M, Medial.

573

574 **Figure 3. Shh responsive genes are misregulated in *Smo*^{ecko} embryos at E10.5.** In
575 situ hybridization of Shh responsive genes on transverse sections through control and
576 *Smo*^{ecko} otic vesicles (n≥3 for all panels) at E10.5. Expression in control embryos (red
577 arrowhead) for most genes is downregulated in *Smo*^{ecko} mutants with the exception of
578 select genes (*Eya1, Eya4, Six1, Jag1*), which show maintained or ectopic expression on
579 the lateral side of the otic vesicle. Scale bar: 100 μm.

580

581 **Figure 4. Shh responsive genes are ectopically expressed in *Shh-P1* embryos.**
582 Schematic of a transverse section through the inner ear of a *Shh-P1* embryo (E11.5)

583 showing ectopic *Shh* expression in the dorsal otocyst (red). In situ hybridization of *Shh*
584 and Shh responsive genes on transverse sections through inner ears of *Shh-P1*
585 embryos at E11.5 (n≥3 for all panels). Ectopic expression is indicated (blue arrowhead).
586 Note that lateral wall genes (*Otx2*, *Capn6* and *Rspo2*) are not influenced by ectopic Shh
587 signaling in *Shh-P1* embryos. Scale bar: 100 μm.
588
589 **Figure 5. ATAC-seq identifies sites of open chromatin at inner ear regulatory**
590 **sequences.** (A) Genomic distribution of ATAC-seq peaks identified in the inner ear at
591 E11.5 (FDR<0.01). (B) ATAC-seq signal enrichment on active versus inactive promoters
592 at E11.5 (*p <0.05, Fisher's exact test). (C) ATAC-seq signal enrichment on mouse
593 (mm) and human (hs) enhancers active in the inner ear, hindbrain and limb from the
594 VISTA enhancer browser (*p<0.05, Fisher's exact test). (D-G) ATAC-seq signal at
595 representative mouse (D,F) and human (E,G) inner ear enhancers from the VISTA
596 enhancer browser. X-gal staining is detected in the otic vesicle (red arrow) of embryos
597 (E11.5) carrying indicated reporter constructs. (H) Comparison of ATAC-seq sequence
598 conservation (PhyloP score) from inner ear, hindbrain and limb between placental
599 mammals and vertebrates. Exonic sequence from the inner ear was used as a deep
600 conservation control (***p <2.2e-16, Kolmogorov-Smirnoff test). Error bars represent
601 standard error of the mean.
602
603 **Figure 6. Identification of Shh dependent inner ear enhancers.** (A) Heatmaps
604 represent the overlap of ATAC-seq (E11.5 inner ear), Gli2 ChIP-seq (E10.5 head), and
605 H3K27ac ChIP-seq (E11.5 hindbrain, ENCODE project, ENCSR129LAP) signals. (B)
606 Venn diagram represents the intersection of ATAC-seq (intergenic and intronic), Gli2-
607 ChIP-seq and H3K27ac-ChIP-seq sites. (C) Gene set enrichment analysis showing
608 significant enrichment of Shh activated genes in the vicinity of overlapping ATAC-seq
609 and Gli2 ChIP-seq peaks (FDR q-value=0.052). (D) HOMER motif enrichment analysis
610 for intersected ATAC-seq and Gli2 ChIP-seq peaks. (E and F) ChIP-qPCR analyses
611 showing significant co-recruitment of Gli2 and Six1 at candidate inner ear enhancers in
612 the vicinity of Shh responsive genes (*p<0.05, Student's t-test). Error bars represent
613 standard error of the mean.

Figure 7. *In vivo* validation of inner ear enhancers. (A,C,E) UCSC genome browser tracks display regions of open chromatin, Gli2 binding and H3K27ac enrichment in the vicinity of Shh responsive genes (*Jag1, Pls1 and Brip1*). Boxed regions (red) represent location of inner ear enhancers. (B,D,F) X-gal staining of transgenic embryos with lacZ reporter constructs driven by IEEs. The number of embryos showing reporter activity in the otic vesicle (red circle) over the total number of transgenic embryos is depicted for each IEE. (B', D', F') Transverse sections through the otic vesicle of representative transgenic embryos at E11.5 reveals a pattern of X-gal staining that is comparable to the expression of the nearby gene (B'', D'', F''). (G) ChIP qPCR analysis of Gli2 binding on IEEs. A *Ptch1* enhancer is included as a positive control (*p<0.05, Student's t-test). Error bars represent standard error of the mean.

ATAC-seq peaks (chromosome coordinates)	Nearest gene	Gli2 ChIP-seq (head)	Presence of Gli motif	Transgenic embryos (n)	Inner ear reporter activity (n)
Chr2:136,932,702-136,936,730	Jag1	Yes	Yes	6	4
Chr9:95,713,880-95,717,088	Pls1	No	Yes	6	4
Chr11:85,972,172-85,973,065	Brip1	No	Yes	7	4
Chr14:9,163,756-9,164,848	Fam107a	No	No	9	0
Chr7:59,140,441-59,141,435	Gas2	No	No	8	0

Table 1. Results of *in vivo* mouse transgenic reporter assay for putative inner ear enhancers in the vicinity of Shh responsive genes.

Figure 1

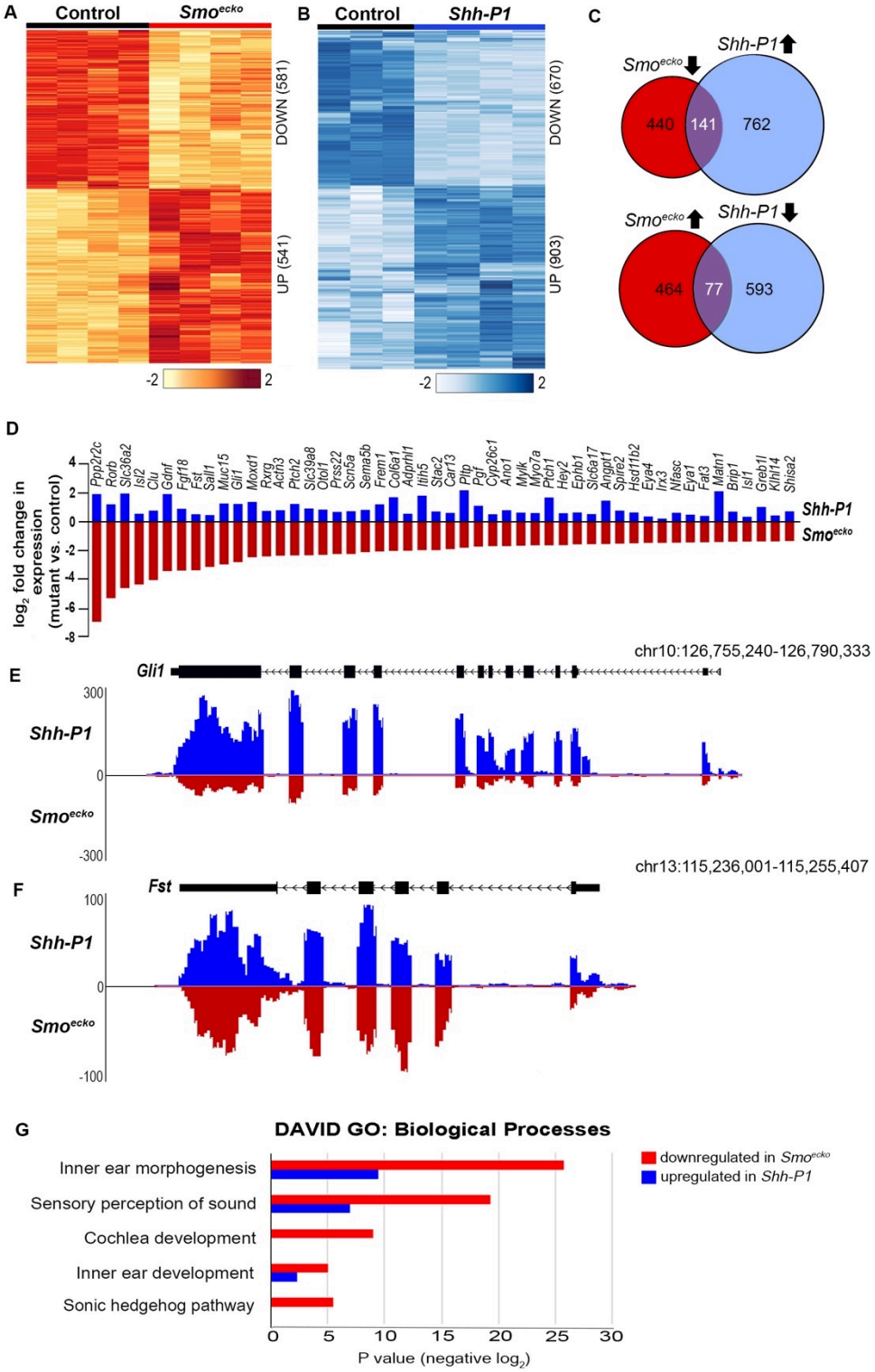

Figure 2

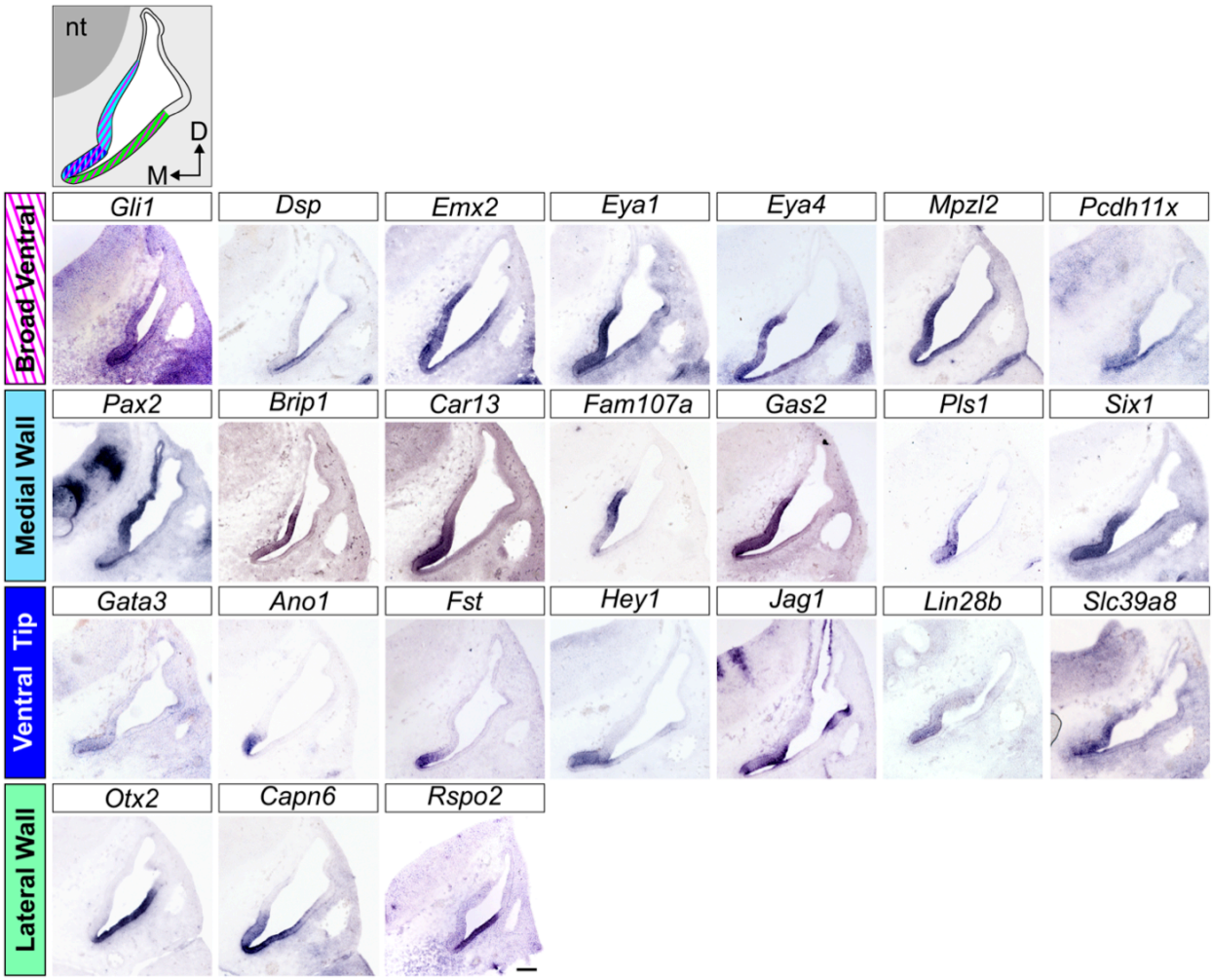

Figure 3

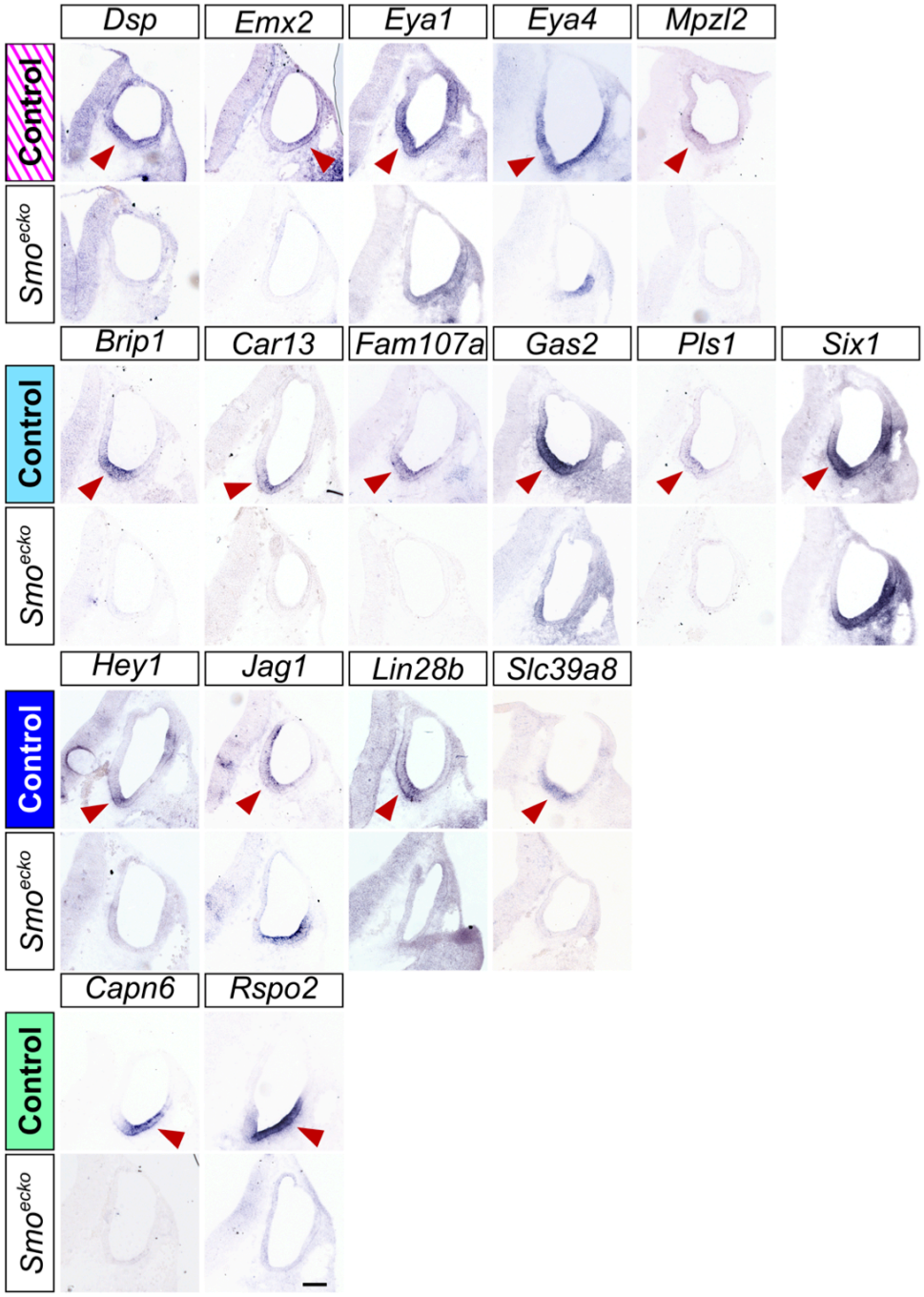

Figure 4

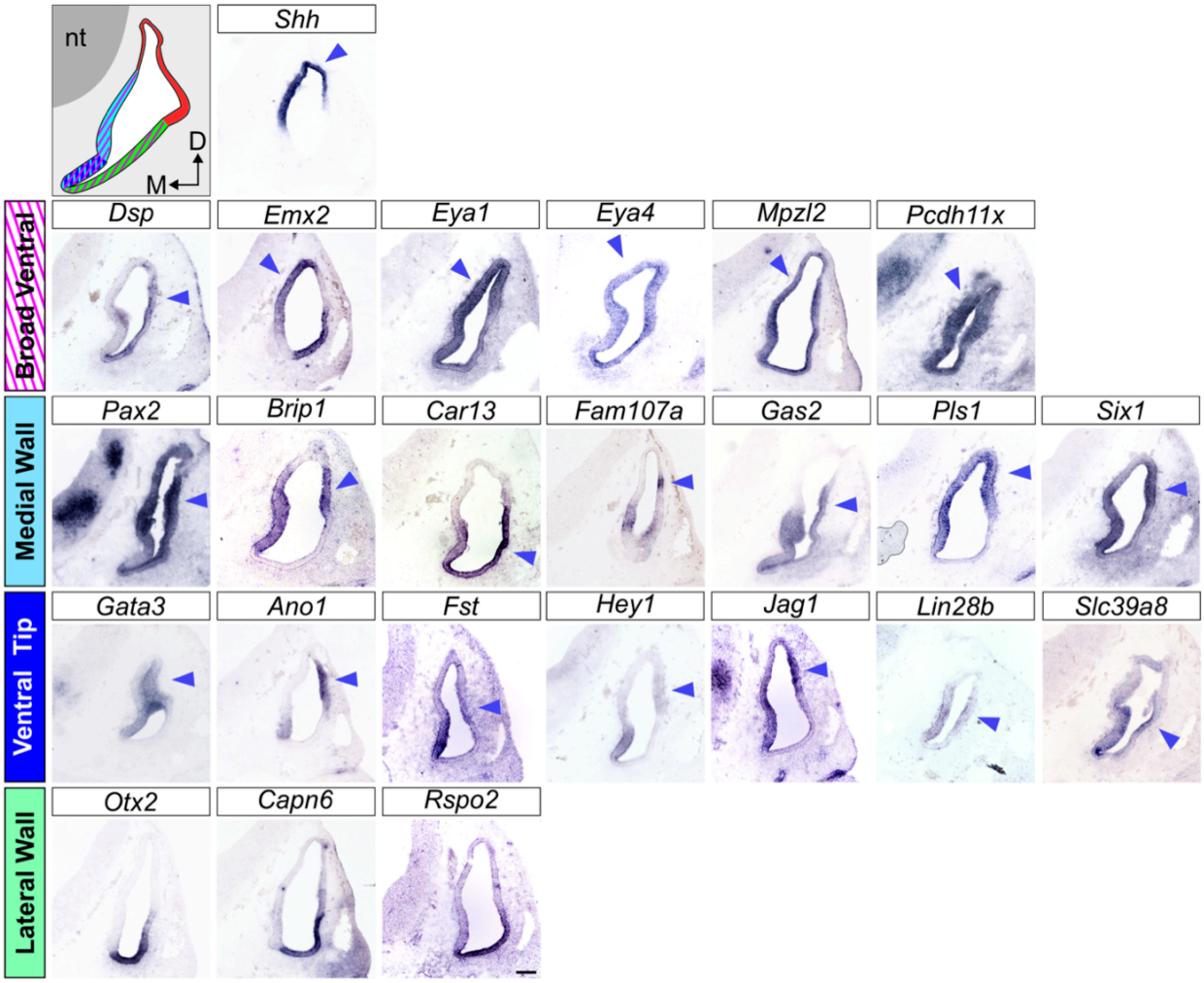

Figure 5

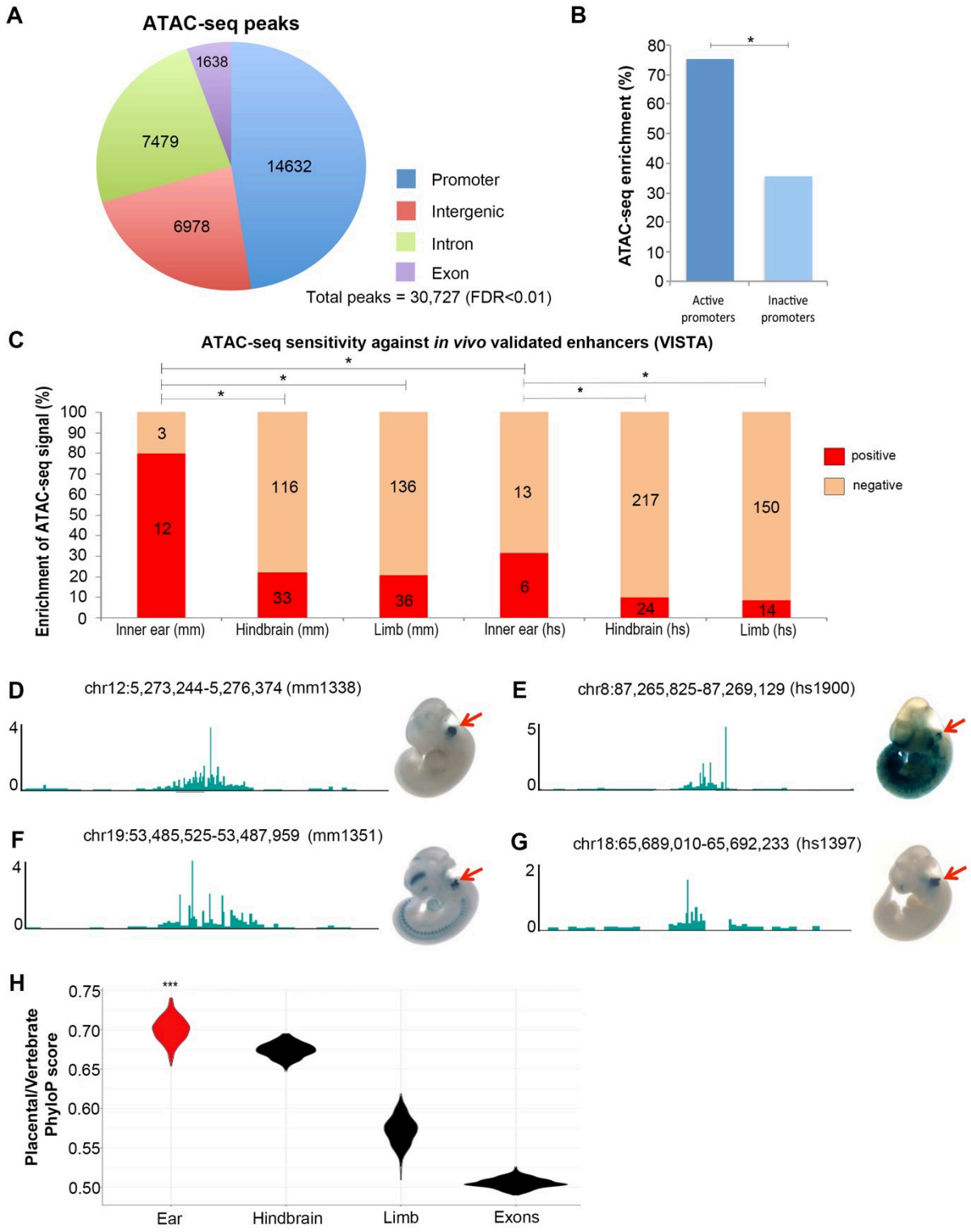

Figure 6

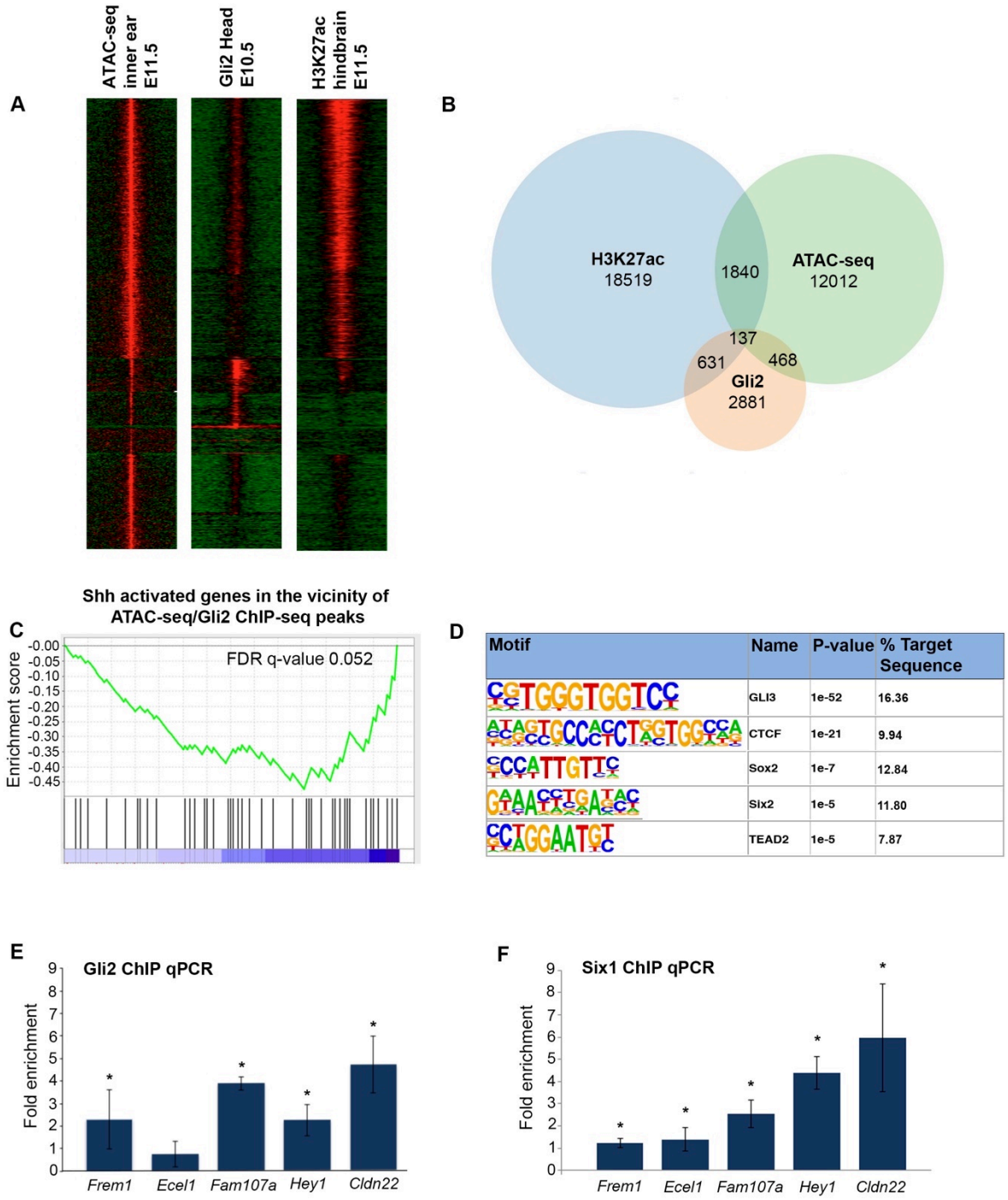

Figure 7